# Incorporating Sodium to Boost the Activity of Aluminium TrenSal Complexes towards racLactide Polymerisation

EurJIC
European Journal of Inorganic Chemistry

Research Article
doi.org/10.1002/ejic.202200134

Chemistry Europe
European Chemical Societies Publishing

www.eurjic.org

# Incorporating Sodium to Boost the Activity of Aluminium TrenSal Complexes towards *rac*-Lactide Polymerisation

Yali Zhou,[a] Gary S. Nichol,[a] and Jennifer A. Garden*[a]

Four novel homo- and heterometallic sodium and/or aluminium complexes based on the TrenSal ligand, **[LH$_3$]**, have been synthesised and fully characterised, including by single-crystal X-ray diffraction experiments. While **[LAl]** was completely inactive towards *rac*-lactide ring-opening polymerisation, incorporating sodium to form heterometallic **[LNaAlMe]** changes the aluminium geometry from octahedral to tetrahedral, leading to good catalytic activity in the presence of co-initiator BnOH ($k_{obs} = 3.19 \times 10^{-2}$ min$^{-1}$; room temperature, toluene solvent) and good polymerisation control. Under identical conditions, homometallic sodium complexes showed higher activities in *rac*-lactide polymerisation than **[LNaAlMe]**, with **[LNa$_3$]** being extremely active ($k_{obs} = 1.21$ min$^{-1}$) but displaying unusual second-order monomer dependency and poor polymerisation control. $^1$H NMR spectroscopic studies suggest that polymerisation with **[LNaAlMe]** or **[LH$_2$Na]**/BnOH follows an activated monomer mechanism, whereas **[LNa$_3$]** operates *via* simultaneous coordination-insertion and activated monomer mechanisms. Overall, heterometallic **[LNaAlMe]** provides a balance of good activity and control compared to the homometallic analogues.

## Introduction

The development of bioderived and biodegradable polymers is an attractive route to decrease societal reliance on petrochemical resources and mitigate the environmental impact of plastics.[1–3] Polylactic acid (PLA) is one of the most prevalent bioderived polymers, with commercial applications in packaging and medicine due to its biorenewability, biodegradability and biocompatibility.[4,5] PLA is generally produced *via* lactide ring-opening polymerisation (LA ROP); this process is crucially dependent on a suitable and efficient catalyst system, and some of the most effective are organometallic catalysts.

Heterometallic (mixed-metal) cooperativity has emerged as a method of enhancing catalyst performance in LA ROP.[6–9] In general, the most significant reactivity enhancements have been observed when pairing a large and Lewis acidic metal (e.g. Group 1 or Ln) with a softer, more carbophilic metal (e.g. Mg or Zn).[10] However, not all heterocombinations display cooperative activity enhancements. The factors which control heterometallic cooperativity are still not well understood in LA ROP, making it difficult to predict heterometallic catalyst performance. This is especially true for Group 1/Al heterocombinations. The commercially available reagent Red-Al, formulated as $Na^+[AlH_2(OCH_2CH_2OCH_3)_2]^-$, displayed low activities in LA ROP under harsh conditions (110-135 °C), which has been attributed to high levels of aggregation.[11] The use of ligands can generally decrease the aggregation state, produce well-defined complexes and enhance solubility. To date, eight alkali metal/aluminium complexes have been reported for LA ROP, yet only two have outperformed their homometallic counterparts.[12–14]

Alkali metals and aluminium are attractive choices in LA ROP due to their low cost, low toxicity, lack of colour and Earth abundance, yet both currently have limitations. Alkali metal complexes tend to display exceptionally high catalyst activities yet often give poor polymerisation control.[15–17] In contrast, aluminium complexes often display good (stereo)control but with relatively low catalytic activities.[18] Combining organoalkali metal and organoaluminium reagents in a 1:1 ratio produces alkali metal (AM) aluminates of general formula $AM^+[AlR_4]^-$ (typically where AM is Li, Na or K, and R is an alkyl or amido group). The anionic formulation of the Al "ate" unit, $[AlR_4]^-$, can boost the nucleophilicity of the organo groups towards CH activation, yet the formation of aluminate complexes can have a "Jekyll" or "Hyde" effect in LA ROP.[12–14]

The only two cooperative alkali metal aluminates reported for LA ROP to date are bis-alkoxide lithium aluminates developed by Dagorne and co-workers (Figure 1).[12] Unusually for aluminium-based ROP catalysts,[19] these complexes displayed good activities at room temperature. In contrast, the homometallic components (LiOBn and LAlOBn, where L = (RNH-*o*-$C_6H_4)_2O$, R = $C_5H_9$ or Cy) were inactive when used separately, as were the mono-alkoxide analogues $[LAl(H)(OBn)Li(THF)_2]$. The authors tentatively proposed that the bis-alkoxide lithium aluminates partially dissociate into LiOBn and LAlOBn during ROP, with LAlOBn activating the monomer and LiOBn acting as the nucleophile source. In a similar vein, Williams and co-workers recently reported a cooperative potassium aluminate

[a] *Y. Zhou, Dr. G. S. Nichol, Dr. J. A. Garden*
*EaStCHEM School of Chemistry*
*University of Edinburgh*
*Joseph Black Building, David Brewster Road, Edinburgh, UK, EH9 3FJ, UK*
*E-mail: j.garden@ed.ac.uk*
http://www.chem.ed.ac.uk/staff/academic-staff/dr-jennifer-garden

*Supporting information for this article is available on the WWW under https://doi.org/10.1002/ejic.202200134*

*Part of the "EurJIC Talents" Special Collection.*

Research Article
doi.org/10.1002/ejic.202200134



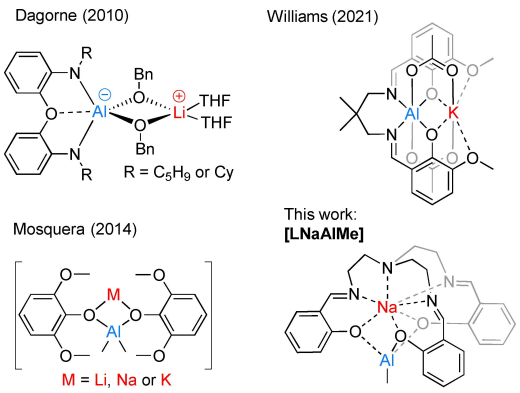


**Figure 1.** Alkali metal aluminates reported for LA ROP (Dagorne, Mosquera) and epoxide/anhydride ROCOP (Williams) and the alkali metal aluminate complex reported in this work.

catalyst for epoxide/anhydride ring-opening copolymerisation (Figure 1),[20] with DFT studies showing that Al coordinates the epoxide monomer whilst ring-opening occurs from the K-$O_{carboxylate}$ nucleophile. These studies indicate that available monomer coordination sites at Al may be key, even in the presence of an alkali metal that could act as a weak Lewis acid for monomer activation.

Other alkali metal aluminates explored as LA ROP catalysts have either matched the activities of the homometallic aluminium analogues (such as the lithium aluminate reported by Mosquera and co-workers, Figure 1), or have displayed much lower activities.[13,14] While the reason for the general decrease in activity with alkali metal aluminates in LA ROP remains unclear, the activity of organoaluminium reagents is known to stem either from the Lewis acidity of Al, or the nucleophilic nature of the organo groups. With some aluminate complexes, monomer coordination sites at Al may be disfavoured both sterically (due to coordinative saturation) and electronically (due to the anionic Al formulation).

Our goal was therefore to synthesise alkali metal aluminates with monomer coordination sites available at Al. We selected the tripodal TrenSal ligand, as this heptadentate ligand contains two distinct binding pockets ($N_4$ and $O_3$, Figure 1) and has some precedent in the synthesis of heterometallic complexes.[21] We hypothesised that this ligand may bind the harder $Al^{3+}$ centre in the outer pocket ($O_3$), and thus generate accessible monomer coordination sites at Al. Herein, we describe the synthesis and characterisation of four novel homometallic and heterometallic Na/Al complexes. The influence of metal upon the Al geometry was probed by X-ray diffraction, and related to the performance of these complexes in *rac*-LA ROP.

## Results and Discussion

### Synthesis and characterisation

The TrenSal ligand, **[$LH_3$]**, was synthesised following a Schiff-base literature protocol.[21] Trivalent (Al) and monovalent (Na) metals were separately or simultaneously incorporated into the ligand scaffold to form monometallic or heterometallic complexes, respectively (Scheme 1). The mono-aluminium complex **[LAl]** was synthesised by deprotonating **[$LH_3$]** with 1 equivalent of $Al(Me)_3$ at 100 °C. Attempts to incorporate a second Al centre, by changing the **[$LH_3$]**:$Al(Me)_3$ stoichiometry to 1:2, still generated **[LAl]** along with unreacted $Al(Me)_3$. Heterometallic **[LNaAlMe]** was selectively synthesised by sequential deprotonation with NaH at room temperature followed by $Al(Me)_3$ at 100 °C. In contrast, reversing the order of addition gave mostly **[LAl]** while adding the two metal reagents simultaneously gave **[LNaAlMe]** but with **[LAl]** formed as a side-product. The selective synthesis of **[LNaAlMe]** required high temperature, as

Yali Zhou graduated with an MSc in Medicinal and Biological Chemistry from the University of Edinburgh (2018). In the same year she started her PhD studies under the supervision of Dr Jennifer Garden. Her research focuses on the design and synthesis of novel homo- and heterometallic catalysts for the ring-opening polymerisation of cyclic esters.

A native of Sunderland, Gary Nichol obtained his PhD from Newcastle University followed by five years at the University of Arizona as the supervisor of the X-ray Diffraction Facility in the (then) Department of Chemistry. In 2011 he moved to Edinburgh University where he oversees a productive crystallography laboratory which includes regular, remote access to beam line I-19 at Diamond Light Source. He is a retired co-editor of Acta Crystallographica Section E.

Jennifer Garden received her MSci (1st Class Hons, 2010) and PhD (2014) from the University of Strathclyde, the latter under the direction of Prof. Robert Mulvey. This was followed by two years as a postdoctoral researcher in the group of Prof. Charlotte Williams at Imperial College London. In 2016, Jennifer moved to the University of Edinburgh as the first recipient of the Christina Miller Research Fellowship, which was followed by a Ramsay Memorial Trust Fellowship (2018–2020), L'Oréal-UNESCO for Women in Science UK & Ireland Fellowship (2019) and UKRI Future Leaders Fellowship (2020-present). Research in the Garden Group combines different fields of chemistry including catalyst development and sustainable polymer synthesis. Jennifer currently sits on the Editorial Advisory Board of ACS Macromolecules and her work has been recognised by awards including the Macro Group UK Young Researchers Medal and the RSC Dalton Division Sir Edward Frankland Fellowship.

Research Article
doi.org/10.1002/ejic.202200134


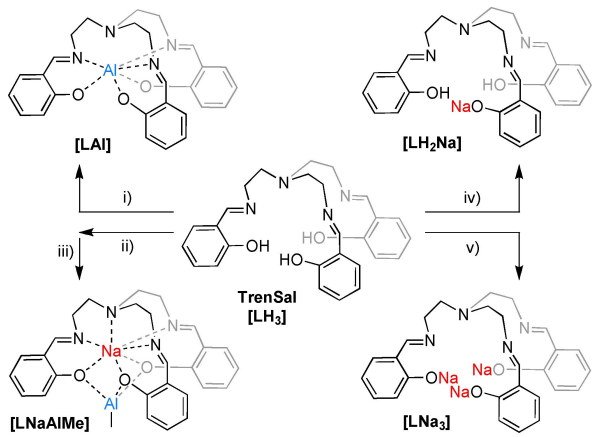


**Scheme 1.** Synthesis of TrenSal complexes **[LAl]**, **[LNaAlMe]**, **[$LH_2Na$]** and **[$LNa_3$]**. Reaction conditions: (i) 1 eq. $Al(Me)_3$, toluene, 3 h, 100 °C, 97.6%; (ii) 1 equiv. NaH, toluene, 1 h, R.T.; (iii) 1 eq. $Al(Me)_3$, toluene, 3 h, 100 °C, 81.7%; (iv) 1 eq. NaHMDS, toluene, 16 h, R.T., 88.9%; (v) 3 eq. NaHMDS, toluene, 16 h, R.T., 86.6%.

a mixture of products was obtained at room temperature. Both **[LAl]** and **[LNaAlMe]** were characterised by X-ray diffraction, multinuclear NMR spectroscopy, mass spectrometry and elemental analysis. The $^1$H NMR spectra for both complexes showed loss of the phenol –OH resonance (13.62 ppm) and chemically equivalent phenoxide rings. This suggests that the solution-state structures are symmetric, which corresponds to the solid-state structures (Figure 2).

Single crystals of **[LAl]** and **[LNaAlMe]** suitable for X-ray diffraction experiments were obtained from toluene solvent at −34 °C (Figure 2, Tables S1–S3, refer to ESI for details). Both molecular structures have $C_3$ symmetry but **[LAl]** is monoclinic and belongs to space group *C*2/*c* while **[LNaAlMe]** is triclinic and belongs to space group *P*-1. The molecular structure of **[LAl]** features a central aluminium centre coordinated by an $N_3O_3$ TrenSal ligand, leaving N4 uncoordinated. Aluminium adopts a distorted octahedral geometry with all N/O–Al–N/O angles close to the ideal bond angles of 90 and 180° (84.79(3)–93.33(3)° and 175.64(3)–176.94(3)° respectively, Table S2). Aluminium is coordinatively saturated, and the octahedral structure implies a lack of space for the incorporation of a second (or third) metal, which corresponded with unsuccessful attempts to incorporate additional Al centres featuring Al–Me units as

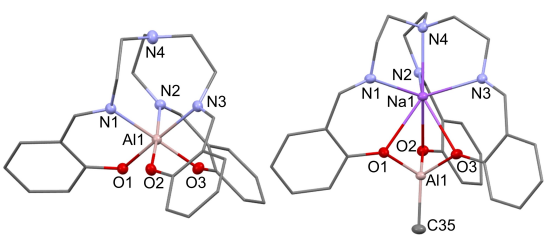


**Figure 2.** Molecular structures of **[LAl]** (left) and **[LNaAlMe]** (right) with thermal ellipsoids drawn at the 50% probability level. Hydrogen atoms and solvents are omitted for clarity.

potential initiating groups. Once formed, **[LAl]** also did not react with organoalkali metal reagents NaH, LiHMDS, NaHMDS or KHMDS under the range of conditions tested (toluene or THF; 0 °C, R.T. or 100 °C). This coordinatively saturated Al geometry may also contribute to the stability of the complex towards air and moisture; exposing **[LAl]** powder to air overnight and monitoring by NMR spectroscopy ($d_6$-DMSO) showed virtually no change to the spectrum (Figure S16, refer to ESI for details).

In the molecular structure of **[LNaAlMe]**, sodium is hepta-coordinated ($N_4O_3$) by the TrenSal ligand, rather than the $N_3O_3$ coordination mode observed for **[LAl]**. This is attributed to the larger ionic radii and thus greater coordination number available for sodium ($Na^+$ = 102 pm and is typically 6–8 coordinate; $Al^{3+}$ = 53 pm and is typically 4–6 coordinate).[22] Aluminium resides in the outside ($O_3$) pocket, coordinating to a methyl group and three phenoxide O atoms with a tetrahedral environment ($\tau_4$ = 1.0, a geometric parameter to distinguish between a perfect square planar geometry ($\tau_4$ = 0) or a tetrahedral geometry ($\tau_4$ = 1) for tetracoordinate metals).[23] Atoms of the apical nitrogen, sodium, aluminium and methyl carbon (C35) are almost linear [N–Na–Al 178.31(4)°, Na–Al–Me 177.18(7)°, Table S3], generating a central axis within the molecule. The Al–O bond distances (1.759(1)–1.767(1) Å) were slightly shorter than those in monometallic **[LAl]** (1.8386(5)–1.8495(5) Å), which implies stronger Al–O bonds and the formation of an "ate" complex.[10] The syntheses of heterometallic complexes **[LLiAlMe]** and **[LKAlMe]** were also investigated using similar reaction conditions (LiHMDS or KHMDS in toluene solvent at R.T., followed by $Al(Me)_3$ at 100 °C). However, both reactions generated a mixture of products after 3 hours, which rearranged to form **[LAl]** overnight, unlike the formation of **[LNaAlMe]**. This was attributed to the suitable size of the sodium ion ($Na^+$ = 102 pm) for the inner pocket of the ligand. The potassium ion ($K^+$ = 138 pm) may be too large to insert into the ligand along with aluminium, and the lithium ion ($Li^+$ = 76 pm) may be too small to coordinate effectively to both N and O atoms.[22] While the ionic radius of lithium is larger than aluminium, the +3 oxidation state of aluminium and mono-metallic structure may contribute to the stable structure of **[LAl]**.

The mono- and tris-sodium complexes **[$LH_2Na$]** and **[$LNa_3$]** were synthesised by the addition of 1 or 3 equivalents of NaHMDS to **[$LH_3$]**, respectively (toluene solvent, R.T., Scheme 1). $^1$H NMR spectroscopic analysis suggested that **[$LNa_3$]** is asymmetric in $d_8$-toluene but symmetric in Lewis donor solvents $d_8$-THF and $d_6$-DMSO, whereas **[$LH_2Na$]** is symmetric in all three deuterated solvents (Figures S11–S12). This difference in the $^1$H NMR spectra could be explained by the DOSY NMR results, which indicate that **[$LH_2Na$]** is a monomer while **[$LNa_3$]** is a tetramer in $d_8$-toluene solution (Figures S14–S15). Aggregation of **[$LNa_3$]** was also indicated by APPI-MS analysis, where signals corresponding to dimers and trimers were observed. However, both sodium complexes were challenging to crystallise and unfortunately, crystals of suitable quality for X-ray diffraction studies could not be obtained. Aggregation is likely to occur through bridging intermolecular Na–O–Na interactions between **[$LNa_3$]** units; such structural motifs have previously been

Research Article
doi.org/10.1002/ejic.202200134



**Table 1.** Polymerisation data for *rac*-LA with complexes **[LAl]**, **[$LH_2Na$]**, **[$LNa_3$]** and **[LNaAlMe]** in the presence or absence of co-initiator BnOH.[a]

| Entry | Catalyst | Time [min] | Conv.[b] [%] | $M_{n,calc}$[c] (1 Chain) [g mol$^{-1}$] | $M_{n,calc}$[c] (2 Chains) [g mol$^{-1}$] | $M_{n,obs}$[d] [g mol$^{-1}$] | | $Đ$[d] | | $P_s$[e] |
|---|---|---|---|---|---|---|---|---|---|---|
| 1 | **[LAl]** | 30 | 0 | – | – | – | | – | | – |
| 2 | **[$LH_2Na$]** | 10 | 76 | 10990 | 5490 | 8470 | | 1.75 | | 0.44 |
| 3[f] | **[$LH_2Na$]** | 10 | 0 | – | – | – | | – | | – |
| 4 | **[$LNa_3$]** | 4 | 83 | 12010 | 6010 | 9100 | 67900[h] | 2.00 | 1.41[h] | 0.48 |
| 5[f] | **[$LNa_3$]** | 3 | 25 | 3570 | 1790 | – | | – | | – |
| 6 | **[LNaAlMe]** | 10 | 42 | 6030 | 3010 | 4290 | | 1.25 | | – |
| 7 | **[LNaAlMe]** | 30 | 65 | 9330 | 4670 | 6730 | | 1.35 | | – |
| 8 | **[LNaAlMe]** | 40 | 77 | 11130 | 5570 | 7060 | | 1.49 | | 0.54 |
| 9[f] | **[LNaAlMe]** | 40 | 4 | 690 | 340 | – | | – | | – |
| 10[g] | **[LNaAlMe]** | 40 | 81 | 11590 | 5800 | 7450 | | 1.93 | | – |

[a] Reaction conditions: [cat.]:[BnOH]:[*rac*-LA] = 1 : 1 : 100, [*rac*-LA] = 1 M in toluene at R.T. [b] Conversion calculated using $^1$H NMR spectroscopy. [c] $M_{n,calc} = M_0 \times ([M]/[I]) \times$ conversion. [d] $M_{n,obs}$ and $Đ$ determined by SEC using polystyrene standards in THF. Values corrected by Mark-Houwink factors (0.58).[27] [e] Determined by homodecoupled $^1$H NMR spectroscopy. [f] Proceeded in the absence of BnOH. [g] Reaction performed in THF. [h] A bimodal distribution was observed.

observed for other sodium alkoxide aggregates and TrenSal complexes.[21,24–26]

### Ring-opening polymerisation of *rac*-lactide

The catalytic activity of homo- and heterometallic complexes **[LAl]**, **[$LH_2Na$]**, **[$LNa_3$]** and **[LNaAlMe]** towards *rac*-LA ROP was investigated using a [catalyst]:[BnOH]:[*rac*-LA] ratio of 1 : 1 : 100 at room temperature. Complexes **[LNaAlMe]**, **[$LH_2Na$]** and **[$LNa_3$]** displayed catalytic activity, whereas homometallic **[LAl]** was inactive (Table 1, entry 1). The poor reactivity of **[LAl]** was attributed to the stable octahedral structure, where the central atom is coordinatively saturated, disfavouring monomer coordination. The inclusion of sodium in **[LNaAlMe]** alters the aluminium geometry, opening up coordination sites at the aluminium centre and thus enhancing monomer coordination. Toluene was selected as the polymerisation solvent after optimising the reaction conditions (Table S4), on the basis of improved polymerisation control *versus* THF ($Đ$ = 1.25–1.61 in toluene *versus* $Đ$ = 1.28–2.28 in THF).

Kinetic studies showed that **[LNaAlMe]** and **[$LH_2Na$]** displayed a first-order dependence on monomer concentration in toluene solvent. Homometallic **[$LH_2Na$]** displayed higher catalytic activities than **[LNaAlMe]**, with respective $k_{obs}$ values of $1.38 \times 10^{-1}$ min$^{-1}$ and $3.19 \times 10^{-2}$ min$^{-1}$ (Figure 3, top; Table S5, entries 3–7 and 17–21). In contrast, the polymerisation with homotrimetallic **[$LNa_3$]** exhibited an unusual second-order dependence on LA concentration, as determined by the linear plot of $1/[LA]_t$ *versus* time (Figure 3, bottom; Table S5, entries 9–15). The second-order dependence on monomer concentration is uncommon but not unprecedented, and is consistent with a mechanism featuring two LA monomers per catalyst.[28,29] **[$LNa_3$]**-assisted polymerisation (4 min, 83 % conversion) is much faster than that based on **[$LH_2Na$]** (5 min, 51 %) and **[LNaAlMe]** (10 min, 42 %). The enhanced activity of **[$LNa_3$]** is attributed to the greater number (and potentially accessibility) of the metal centres in **[$LNa_3$]** (*versus* **[LAl]**, **[LNaAlMe]** and **[$LH_2Na$]**). Sodium (and indeed other alkali metal) complexes typically display very high catalytic activities in *rac*-LA ROP, yet often give poor

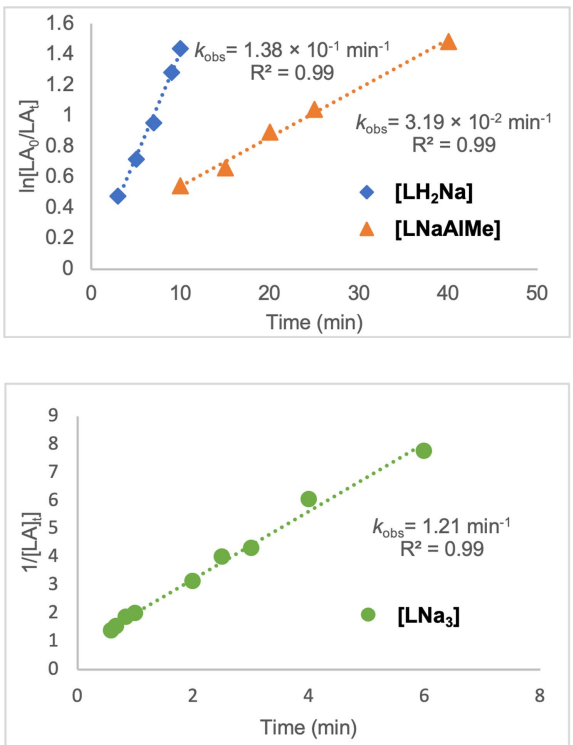


**Figure 3.** Top: first-order kinetic plot for *rac*-LA *versus* time using **[$LH_2Na$]**/BnOH or **[LNaAlMe]**/BnOH as an initiator. Bottom: second-order kinetic plot for *rac*-LA *versus* time using **[$LNa_3$]**/BnOH as an initiator. Reaction conditions: R.T. with catalyst in toluene solvent with loading ratio of [cat]:[BnOH]:[*rac*-LA] = 1 : 1 : 100.

control over the molecular weight and dispersity.[17] Previous studies have suggested that alkali metal complexes can simultaneously operate through two different LA ROP mechanisms (coordination-insertion and activated monomer) in the presence of an exogeneous alcohol, a factor which may be partially responsible for the poor polymerisation control.[15,16] Indeed, poor control occurs with **[$LNa_3$]**; a bimodal distribution and broad dispersities are observed after 50 s (Table 1, entry 4; Table S5, entries 9–15). Narrower dispersities were generally obtained with **[$LH_2Na$]** yet these values increased in the late

Research Article
doi.org/10.1002/ejic.202200134


stages of the reaction, which was attributed to transesterification ($Đ = 1.75$, Table 1, entry 2; Table S5, entries 3–7). The $M_{n,obs}$ values of PLA generated by **[LH$_2$Na]** generally showed a relatively good agreement with the $M_{n,calc}$ values for one chain per catalyst until the late stages of the reaction (Table S5, entries 3–7). The polymerisation control was generally improved using heterometallic **[LNaAlMe]** ($Đ = 1.25$–$1.49$, Table 1, entries 6–8), which gave narrower dispersities, a monomodal SEC trace and a linear relationship between $M_{n,obs}$ and monomer conversion, albeit with the $M_{n,obs}$ values falling in between the $M_{n,calc}$ values for 1 and 2 chains initiated per catalyst (Graph S1, refer to ESI for details). This may be explained by intra- and intermolecular transesterification reactions, which were observed by MALDI-ToF analysis in the later stages of the reaction ($\Delta$ (m/z) = 72 g mol$^{-1}$, Figure S17). No stereocontrol was observed with **[LH$_2$Na]**, **[LNa$_3$]** and **[LNaAlMe]** as atactic PLA was generated ($P_s \approx 0.5$, Table 1).

To understand the initiation mechanism, control reactions were performed using **[LNaAlMe]** in the absence of co-initiator BnOH, which generated only traces of PLA (Table 1, entry 9). This indicates that the Al–Me bond of **[LNaAlMe]** does not initiate ROP. $^1$H NMR spectroscopic analysis suggests that the Al–Me group of **[LNaAlMe]** is less polarised than that of Al(Me)$_3$, on the basis that the –*C*H$_3$ resonances are shifted downfield for **[LNaAlMe]** (0.02 ppm in $CDCl_3$) compared to Al(Me)$_3$ (−0.69 ppm in $CDCl_3$). These observations suggest that the formation of aluminate complexes does not necessarily increase the polarity (thus Brønsted basicity or nucleophilicity) of Al–C bonds. Control polymerisations were performed with Al(Me)$_3$ in either the presence or absence of 1 equivalent BnOH, and gave no PLA under the reaction conditions investigated, in spite of the increased δ- charge (thus expected increased reactivity) of the Al–Me group (toluene solvent, R.T., Table S5, entries 23–24). These observations suggest that the nucleophilicity of the Al–Me unit does not solely determine reactivity in ROP, and that other factors (such as available coordination sites at Al) are also important. MALDI-ToF analysis showed that using **[LNaAlMe]** with BnOH generated benzoxide end-capped linear PLA and cyclic PLA but no methyl end-capped PLA (Figure S17), providing further evidence that the methyl group of **[LNaAlMe]** does not ring-open *rac*-LA.

To determine whether initiation with **[LNaAlMe]**/BnOH occurred *via* an activated monomer mechanism (where nucleophilic attack of LA occurs from an exogeneous alcohol) or a coordination insertion mechanism (where nucleophilic attack occurs from a metal-alkoxide unit),[15] the reaction between **[LNaAlMe]** and BnOH (1 : 1 ratio) was investigated. For consistency with the polymerisation conditions, the stoichiometric reaction was performed in toluene solvent at room temperature and then analysed in $CDCl_3$ solvent due to the poor solubility of **[LNaAlMe]** in $d_8$-toluene. No obvious shift of the **[LNaAlMe]** resonances was detected, and no methane resonance (δ = 0.22 ppm) was observed (Figure S24).[30] The BnOH resonances also stayed at the same chemical shifts although the benzylic-*C*H$_2$ resonance changed from a singlet (BnOH alone) to a doublet (BnOH and **[LNaAlMe]**), which may arise from BnOH coordination to a metal centre.[9] However, the DOSY analysis did not provide clear support for this observation (Figure S25), as the BnOH and **[LNaAlMe]** resonances showed different diffusion coefficients. The stability of Al-CH$_3$ towards BnOH also emphasises that the addition of sodium does not increase the nucleophilic character of **[LNaAlMe]** as has been reported for other alkali metal aluminates.[31,32] There was also no obvious reaction when **[LNaAlMe]** and *rac*-LA were combined in a 1 : 1 ratio (neither a shift of the LA $^1$H NMR resonances nor ring-opening of *rac*-LA was observed, Figure S24). Combining a 1 : 1 : 1 mixture of **[LNaAlMe]**, BnOH and *rac*-LA generated products that may correspond to the insertion of the ring-opened monomer into BnOH, while **[LNaAlMe]** appears mostly intact at the end of the reaction (Figure S24). Taken together, these reactivity studies suggest the **[LNaAlMe]**-based polymerisation proceeds *via* an activated monomer mechanism, where LA coordinates to **[LNaAlMe]** and then undergoes nucleophilic attack and ring-opening by BnOH. As for mono-sodium catalyst **[LH$_2$Na]**, no *rac*-LA polymerisation occurred in the absence of BnOH (Table 1, entry 3), suggesting that the Na-O$_{ligand}$ bond cannot initiate the polymerisation. This is further supported by the absence of ligand end groups in the MALDI-ToF analysis. Furthermore, **[LH$_2$Na]** does not appear to undergo a significant reaction with BnOH (Figure S27), which suggests **[LH$_2$Na]**/BnOH-catalysed polymerisation also occurred through an activated monomer mechanism with BnOH as the initiator rather than *via* rearrangement to form an active NaOBn species.

Similar mechanistic studies were also performed for tris-sodium catalyst **[LNa$_3$]**, by investigating the 1 : 1 reaction between **[LNa$_3$]** and BnOH. The $^1$H NMR resonances of **[LNa$_3$]** remained unchanged (Figure S28) and DOSY NMR analysis showed different diffusion coefficients for **[LNa$_3$]** and BnOH (Figure S29). These observations suggest that BnOH does not react with **[LNa$_3$]**, and instead, acts as a source of a nucleophile implying an activated monomer mechanism (the same as the **[LNaAlMe]**/BnOH and **[LH$_2$Na]**/BnOH-catalysed systems). To confirm this hypothesis, the reaction of **[LNa$_3$]**, *rac*-LA and BnOH (1 : 1 : 1) was also investigated, from which ring-opening of *rac*-LA was observed with **[LNa$_3$]** still present in solution (Figure S28). However, MALDI-ToF results of PLA generated in the presence of **[LNa$_3$]** and BnOH showed the generation of ligand end-capped PLA in the lower molecular weight range (Figure S19), suggesting **[LNa$_3$]** has potential to initiate the polymerisation *via* the Na–O$_{ligand}$ bond. On the other hand, benzoxide end-capped and cyclic PLA were observed from low to high molecular weight ranges (Figure S19). The cyclic polymers may be formed *via* Na–O$_{ligand}$ initiation followed by intramolecular transesterification reactions, which could regenerate **[LNa$_3$]** as proposed for other alkali metal catalysts.[15,16,33] This suggests that both BnOH and Na–O$_{ligand}$ bond(s) of **[LNa$_3$]** may initiate LA ROP, and thus both activated monomer and coordination-insertion mechanisms may occur simultaneously in the **[LNa$_3$]**/BnOH-assisted polymerisation, as has previously been reported for alkali metal catalysts based on phenoxyimine ligands.[15] A control reaction in the absence of co-initiator BnOH provided further support that **[LNa$_3$]** can initiate the ROP of *rac*-LA without BnOH (Table 1, entry 3), where the polymerisation is proposed to proceed through a coordination-insertion

mechanism, as evidenced by MALDI-ToF data (Figure S20). Indeed, the bimodal distribution observed in the presence of BnOH may arise from the ligand end-capped PLA produced *via* the coordination-insertion mechanism, and the benzoxide end-capped PLA produced *via* the activated monomer mechanism.

Heterometallic **[LNaAlMe]** was also investigated for the ROP of ε-caprolactone (ε-CL) and δ-valerolactone (δ-VL), using the same conditions as for the *rac*-LA studies ([cat.]:[BnOH]:[monomer] = 1 : 1 : 100, toluene solvent, R.T.). Notably, **[LNaAlMe]** displayed much lower activities than in *rac*-LA ROP, with only 9% and 35% conversion of ε-CL and δ-VL observed after 24 hours, respectively (Table S6, entries 3 and 7). With δ-VL, increasing the reaction temperature accelerated the polymerisation rate but also gave broad dispersities, which may be caused by transesterification (Table S6, entries 6, 8 and 9).

## Conclusion

In summary, homometallic (**[LAl]**, **[$LH_2Na$]** and **[$LNa_3$]**) and heterometallic (**[LNaAlMe]**) TrenSal complexes were synthesised and characterised through a combination of multinuclear NMR spectroscopy, mass spectrometry, elemental analysis and X-ray crystallography. Heterometallic **[LNaAlMe]** bears a "closed" structure, and thus differs from previously reported heterometallic Al catalysts for LA ROP, as only one metal (Al) features accessible monomer coordination sites. In the presence of co-initiator BnOH, heterometallic **[LNaAlMe]** and homometallic complexes **[$LH_2Na$]** and **[$LNa_3$]** displayed high catalyst activity, while complex **[LAl]** was inactive. This difference highlights the importance of incorporating Na for accessing catalytic activity, as this alters the geometry of Al from octahedral to tetrahedral and opens up monomer coordination sites. To the best of our knowledge, these studies report the first series of TrenSal-based complexes as catalysts for *rac*-LA ROP.

Reactivity studies indicate that **[LNaAlMe]** follows an activated monomer mechanism, maintaining the methyl group bonded to aluminium and with nucleophilic attack of LA occurring from exogeneous BnOH. Intriguingly, NMR spectroscopy studies suggest that the nucleophilicity of the Al–Me unit is not enhanced through the formation of a heterometallic sodium aluminate species and that instead, the availability of coordination sites at Al is key. While **[LNaAlMe]** displays a slower ROP rate than that of **[$LH_2Na$]** and **[$LNa_3$]**, it gives better control over the polymerisation, as **[$LH_2Na$]** gives polymers with broad dispersity in the late stages of the reaction and **[$LNa_3$]** generates polymers with bimodal distributions. Complex **[$LNa_3$]** also showed an unusual second-order dependence on monomer concentration. The data from control reactions (without BnOH) and MALDI-ToF analysis suggests that with **[$LNa_3$]**, polymerisation may proceed through both coordination-insertion and activated monomer mechanisms. In contrast, **[$LH_2Na$]** and **[LNaAlMe]** display first order kinetics. In heterometallic **[LNaAlMe]**, the multidentate TrenSal ligand offers the potential to block the alkali metal from monomer coordination, thus limiting the available polymerisation pathways and improving the polymerisation control. To enhance future heterometallic catalyst design for LA ROP, other complexes should be investigated that generate understanding of heterometallic cooperativity beyond simply incorporating additional sites for monomer coordination. This will be the subject of ongoing research in our laboratory.

## Experimental Section

All manipulations involving air- or moisture-sensitive compounds were performed under argon atmosphere using standard Schlenk-line techniques and gloveboxes. All reagents were purchased from Sigma-Aldrich, Fisher Scientific, Acros Organics or Fluorochem and were used as received unless stated otherwise. Dry THF and toluene were collected from a solvent purification system (Innovative Technologies) and stored in the presence of activated molecular sieves (4 Å) under argon. Deuterated NMR solvents ($d_8$-toluene, $d_8$-THF and $CDCl_3$) were degassed by three freeze-pump-thaw cycles and stored over activated 4 Å molecular sieves under argon. $d_6$-DMSO NMR solvent was dried by filtration through and storage over activated 4 Å molecular sieves under argon. *Rac*-lactide (*rac*-LA) was purified by double recrystallisation from toluene followed by sublimation under vacuum and was subsequently stored in the glovebox freezer at −34 °C. Benzyl alcohol (BnOH), ε-caprolactone (ε-CL) and δ-valerolactone (δ-VL) were dried over $CaH_2$ and distilled under reduced pressure prior to use.

1D ($^1H$, $^{13}C$) and 2D (COSY, HSQC) and DOSY NMR spectra were recorded on Bruker AVA400, AVA500 and AVA600 spectrometers at 298 K with the chemical shifts referenced to residual solvent resonances. The chemical shifts (δ) are quoted relative to tetramethylsilane. The DOSY plot was generated using the DOSY processing module of TopSpin. Parameters were optimised empirically to find the best quality of data for explanation purposes. Elemental microanalysis was performed by Elemental Microanalysis Ltd. Mass spectrometry (MS) data for ligand was carried out using accurate electrospray ionisation MS in the positive ion mode and collected on a Thermo Fisher Scientific TRACE™ GC Ultra gas chromatograph. Complexes were characterised *via* APPI-MS analysis under a protective nitrogen gas bubbles using a Bruker Daltonics 12T SolariX Fourier Transform Ion Cyclotron Resonance Mass Spectrometer. Molecular weights of polymers were determined by size exclusion chromatography (SEC) in a 1260 Agilent Infinity II GPC/SEC single detection system with mixed bed C PLgel columns (300 × 7.5 mm) and were calibrated using polystyrene standards and corrected by a Mark-Houwink factor of 0.58 for poly(lactic acid).[27] MALDI-ToF mass analysis was performed using a Bruker Daltonics UltrafleXtreme™ MALDI-ToF/ToF MS instrument. Dithranol was used as matrix and potassium iodide was added as a cationising additive.

### Synthesis and characterisation of TrenSal ligand [$LH_3$]

Tris-((2-hydroxybenzylidene)aminoethyl)amine was prepared according to a literature procedure.[21] Salicylaldehyde solution (3.19 mL in 25 mL ethanol, 30 mmol) was slowly added to a solution of tris(2-aminoethyl) amine (1.50 mL in 25 mL ethanol, 10 mmol). The resulting mixture was refluxed for 2 hours, cooled down slowly to room temperature and copious amounts of yellow crystals formed. The resulting yellow crystals were isolated by filtration, washed several times with ethanol, and dried *in vacuo*.

Ligand **[$LH_3$]**: (420.0 mg, 91.6%). $^1H$ NMR (400 MHz, $CDCl_3$) δ 13.76 (s, 3H, OH), 7.83 (d, $J$ = 1.3 Hz, 3H, N=CH), 7.25 (td, 3H, ArH), 6.93 (dd, $J$ = 8.3, 1.1 Hz, 3H, ArH), 6.60 (td, $J$ = 7.5, 1.1 Hz, 3H, ArH), 6.12 (dd, $J$ = 7.7, 1.7 Hz, 3H, ArH), 3.54 (ddd, $J$ = 6.5, 3.7, 1.2 Hz, 6H, $CH_2$),

2.94–2.78 (m, 6H, $CH_2$). $^{13}C$ NMR (101 MHz, $CDCl_3$) δ 166.3 (C=N), 161.3 (C–O), 132.1, 131.9, 118.8, 118.7, 116.9 (ArC), 58.2, 56.1 ($CH_2$). Both spectra gave good agreement with literature values.[21] EI-MS: *m/z* $[M]^+$: 458.23 calculated $[M]^+$: 458.56.

### Synthesis and characterisation of TrenSal Na/Al complex [LNaAlMe]

TrenSal ligand **[$LH_3$]** (458.6 mg, 1 mmol) and NaH (95%, 26.4 mg, 1.1 mmol) were weighed into a Schlenk flask and dissolved in dry toluene (20 mL). The resulting solution was stirred for 1 hour at room temperature and then $Al(Me)_3$ solution (2 M in toluene, 0.50 mL, 1 mmol) was added dropwise. The resulting mixture was subsequently stirred for 3 hours at 100 °C under an argon atmosphere. The solvent was subsequently removed *in vacuo*, resulting in an off-white powder.

Complex **[LNaAlMe]**: (425.3 mg, 81.7%). $^1H$ NMR (500 MHz, $CDCl_3$) δ 8.20 (s, 3H, N=CH), 7.17 (d, $J=7.5$ Hz, 3H), 7.15 (s, 3H, ArH), 6.95 (d, $J=8.1$ Hz, 3H, ArH), 6.72 (td, $J=7.3$, 1.2 Hz, 3H, ArH), 3.71–3.54 (m, 6H, $CH_2$), 2.83–2.70 (m, 6H, $CH_2$), 0.03 (s, 3H, $CH_3$). $^{13}C$ NMR (126 MHz, $CDCl_3$) δ 165.2 (C=N), 160.2 (C–O), 135.4, 131.9, 123.6, 121.0, 117.2 (ArC), 60.5, 55.5 ($CH_2$), 1.2 ($CH_3$). Elemental Analysis: predicted: C 64.61%, H 5.81%, N 10.76%; found: C 64.36%, H 5.80%, N 10.56%. *m/z* (APPI-MS): 521.20 **[LNaAlMe** + H]$^+$ (calc: 521.20).

### Synthesis and characterisation of TrenSal Al complex [LAl]

TrenSal ligand **[$LH_3$]** (458.4 mg, 1 mmol) was weighed into a Schlenk flask and dissolved in dry toluene (20 mL) under argon. $Al(Me)_3$ solution (2 M in toluene, 0.50 mL, 1 mmol) was dropwise added to the ligand solution at room temperature. The resulting mixture was stirred for 3 hours at 100 °C under an argon atmosphere. The solution was subsequently removed *in vacuo*, resulting in a pale-yellow powder.

Complex **[LAl]**: (470.8 mg, 97.6%). $^1H$ NMR (500 MHz, $d_6$-DMSO) δ 8.28 (s, 3H, N=CH), 7.26 (d, $J=1.7$ Hz, 3H, ArH), 7.20–7.17 (m, 3H, ArH), 6.62–6.50 (m, 3H, ArH), 6.39 (d, $J=8.4$ Hz, 3H, ArH), 3.59–3.49 (m, 3H, $CH_2$), 3.26–3.16 (m, 3H, $CH_2$), 3.08 (dd, $J=11.9$, 3.5 Hz, 3H, $CH_2$), 2.92 (td, $J=13.6$, 12.3, 3.6 Hz, 3H, $CH_2$). $^{13}C$ NMR (126 MHz, $d_6$-DMSO) δ 169.5 (C=N), 165.2 (C–O), 134.0, 124.9, 120.5, 118.5, 113.5 (ArC), 61.0, 55.6 ($CH_2$). Elemental Analysis: predicted **[LAl** + 1/5 toluene]: C 68.09%, H 5.75%, N 11.18%; found: C 68.04%, H 5.63%, N 10.93%. *m/z* (APPI-MS): 483.19 **[LAl** + H]$^+$ (calc: 483.20).

### Synthesis and characterisation of TrenSal Na complexes [$LH_2Na$] and [$LNa_3$]

TrenSal ligand **[$LH_3$]** (458.4 mg, 1 mmol) and NaHMDS (183.6 mg, 1 mmol for **[$LH_2Na$]** or 412.8 mg, 3 mmol for **[$LNa_3$]**) were weighed into a Schlenk flask and dissolved in dry toluene (20 mL) in the glovebox. The resulting mixture was stirred for 16 hours at room temperature under an argon atmosphere. The solvent was subsequently removed *in vacuo*, resulting in a yellow powder. In spite of attempts to remove HMDS(H) under vacuum (including at high temperatures), traces of HMDS(H) persisted, as observed by $^1H$ NMR spectroscopy; NaHMDS and **[$LH_3$]** appear to exist in equilibrium with **[$LNa_3$]**, HMDS(H) and **[$LH_2Na$]**.

Complex **[$LH_2Na$]**: (427.2 mg, 88.9%). $^1H$ NMR (500 MHz, $d_6$-DMSO) δ 13.82 (s, 2H, OH), 8.32 (s, 3H, N=CH), 7.13 (td, $J=7.9$, 4.4 Hz, 3H, ArH), 7.08 (dd, $J=7.6$, 1.8 Hz, 3H, ArH), 6.65 (d, $J=8.3$ Hz, 3H, ArH), 6.50 (s, 3H, ArH), 3.56 (t, $J=6.0$ Hz, 6H, $CH_2$), 2.79 (t, $J=6.1$ Hz, 2H, $CH_2$). $^{13}C$ NMR (126 MHz, $d_6$-DMSO) δ 165.3 (C=N), 137.3 (C–O), 131.6, 128.9, 128.2, 125.3, 120.1 (ArC), 58.0, 55.4 ($CH_2$). Elemental Analysis: predicted **[$LH_2Na$** + 1/3 toluene]: C, 68.91%; H, 6.24%; N, 10.96%; found: C 68.69%, H 6.08%, N 10.80%. *m/z* (APPI-MS): 481.21 **[$LH_2Na$** + H]$^+$ (calc: 481.22). **[$LH_3$]** is observed as the major peak, which is attributed to ligand protonation upon exposure to air prior to the sample analysis by APPI-MS. Peaks for **[$LNa_3$]** were also observed and are attributed to proton rearrangement during the mass spectrometry analysis ($3LH_2Na \rightarrow 2LH_3 + LNa_3$).

Complex **[$LNa_3$]**: (534.4 mg, 86.6%). $^1H$ NMR (500 MHz, $d_6$-DMSO) δ 8.11 (s, 3H, N=CH), 6.95 (dd, $J=7.7$, 2.1 Hz, 3H, ArH), 6.81 (d, $J=2.0$ Hz, 3H, ArH), 6.26 (d, $J=8.4$ Hz, 3H, ArH), 5.99 (t, $J=7.2$ Hz, 3H, ArH), 3.43 (t, $J=5.0$ Hz, 6H, $CH_2$), 2.62 (t, $J=5.2$ Hz, 6H, $CH_2$). $^{13}C$ NMR (126 MHz, $d_6$-DMSO) δ 172.4 (C=N), 165.5 (C–O), 134.1, 130.6, 123.0, 122.4, 107.5 (ArC), 59.6, 57.0 ($CH_2$). Elemental Analysis: predicted: C 61.83%, H 5.19%, N 10.68%; found: C 60.07%, H 5.46%, N 9.37%. *m/z* (APPI-MS): 525.18 **[$LNa_3$** + H]$^+$ (calc: 525.18). **[$LH_3$]** is observed as the major peak, which is attributed to ligand protonation upon exposure to air prior to the sample analysis by APPI-MS. Peaks attributed to dimeric {**[$LNa_3$]$_2$** + H}$^+$ (1049.36) and trimeric {**[$LNa_3$]$_3$** + H}$^+$ (1573.54) were also observed.

Deposition Numbers 2152220 (for **[LAl]**) and 2152221 (for **[LNaAlMe]**) contain the supplementary crystallographic data for this paper. These data are provided free of charge by the joint Cambridge Crystallographic Data Centre and Fachinformationszentrum Karlsruhe Access Structures service www.ccdc.cam.ac.uk/structures.

## Acknowledgements

*We gratefully acknowledge the University of Edinburgh Principal's Career Development PhD Scholarship for funding. J. A. G. also acknowledges the UKRI Future Leaders Fellowship (Grant MR/T042710/1), British Royal Society (Grant RSG\R1\180101), L'Oréal-UNESCO for Women in Science UK & Ireland Fellowship, L'Oréal-UNESCO International Rising Talents Award and the British Ramsay Memorial Trust for funding. Synchrotron data were collected remotely at beam line I-19 of Diamond Light Source (award CY22240).*[34]

## Conflict of Interest

The authors declare no conflict of interest.

## Data Availability Statement

The data that support the findings of this study are available in the supplementary material of this article.

**Keywords:** Aluminium · Heterometallic complexes · Lactide · Ring-opening polymerisation · Sodium

[1] J. N. Hahladakis, C. A. Velis, R. Weber, E. Iacovidou, P. Purnell, *J. Hazard. Mater.* **2018**, *344*, 179–199.
[2] F. Shewmaker, M. J. Kerner, M. Hayer-Hartl, G. Klein, C. Georgopoulos, S. J. Landry, *Protein Sci.* **2004**, *13*, 2139–2148.

Research Article
doi.org/10.1002/ejic.202200134


[3] "*Science to Enable Sustainable Plastics – A White Paper from the 8th Chemical Sciences and Society Summit (CS3)*", can be found under rsc.li/sustainable-plastics-report, **2020**.
[4] X. Zhang, M. Fevre, G. O. Jones, R. M. Waymouth, *Chem. Rev.* **2018**, *118*, 839–885.
[5] A. Duda, S. Penczek, *Polimery* **2018**, *48*, 16–27.
[6] Y. Sarazin, R. H. Howard, D. L. Hughes, S. M. Humphrey, M. Bochmann, *Dalton Trans.* **2006**, *60*, 340–350.
[7] W. Gruszka, A. Lykkeberg, G. S. Nichol, M. P. Shaver, A. Buchard, J. A. Garden, *Chem. Sci.* **2020**, *2*, 11785–11790.
[8] H. Y. Chen, M. Y. Liu, A. K. Sutar, C. C. Lin, *Inorg. Chem.* **2010**, *49*, 665–674.
[9] W. Gruszka, H. Sha, A. Buchard, J. A. Garden, *Catal. Sci. Technol.* **2022**, *12*, 1070–1079.
[10] W. Gruszka, J. A. Garden, *Nat. Commun.* **2021**, *12*, 1–13.
[11] H. Li, C. Wang, F. Bai, J. Yue, H. G. Woo, *Organometallics* **2004**, *23*, 1411–1415.
[12] F. Hild, P. Haquette, L. Brelotc, S. Dagorne, *Dalton Trans.* **2010**, *39*, 533–540.
[13] M. T. Muñoz, T. Cuenca, M. E. G. Mosquera, *Dalton Trans.* **2014**, *43*, 14377–14385.
[14] A. J. Gaston, Z. Greindl, C. A. Morrison, J. A. Garden, *Inorg. Chem.* **2021**, *60*, 2294–2303.
[15] Y. Zhou, G. S. Nichol, J. A. Garden, *Eur. J. Org. Chem.* **2021**, *2021*, 5557–5568.
[16] F. M. García-Valle, R. Estivill, C. Gallegos, T. Cuenca, M. E. G. Mosquera, V. Tabernero, J. Cano, *Organometallics* **2015**, *34*, 477–487.
[17] A. K. Sutar, T. Maharana, S. Dutta, C. T. Chen, C. C. Lin, *Chem. Soc. Rev.* **2010**, *39*, 1724–1746.
[18] Y. Naganawa, K. Maruoka in *Modern Organoaluminum Reagents: Preparation, Structure, Reactivity and Use*, Vol.41 (Eds.: S. Woodward, S. Dagorne), Springer, Berlin, Heidelberg, **2012**, pp. 187–214.
[19] S. Gesslbauer, R. Savela, Y. Chen, A. J. P. White, C. Romain, *ACS Catal.* **2019**, *9*, 7912–7920.
[20] W. T. Diment, G. L. Gregory, R. W. F. Kerr, A. Phanopoulos, A. Buchard, C. K. Williams, *ACS Catal.* **2021**, *11*, 12532–12542.
[21] A. Mustapha, K. Busch, M. Patykiewicz, A. Apedaile, J. Reglinski, A. R. Kennedy, T. J. Prior, *Polyhedron* **2008**, *27*, 868–878.
[22] R. D. Shannon, *Acta Crystallogr.* **1976**, *A32*, 751–767.
[23] L. Yang, D. R. Powell, R. P. Houser, *Dalton Trans.* **2007**, 955–964.
[24] W. Clegg, M. G. Davidson, D. V. Graham, G. Griffen, M. D. Jones, A. R. Kennedy, C. T. O'Hara, L. Russo, C. M. Thomson, *Dalton Trans.* **2008**, 1295–1301.
[25] M. P. Hogerheide, S. N. Ringelberg, M. D. Janssen, J. Boersma, A. L. Spek, G. van Koten, *Inorg. Chem.* **1996**, *35*, 1195–1200.
[26] P. I. Binda, B. R. Hill, B. W. Skelton, *J. Coord. Chem.* **2018**, *71*, 941–951.
[27] A. Kowalski, A. Duda, S. Penczek, *Macromol.* **1998**, *31*, 2114–2122.
[28] P. I. Binda, E. E. Delbridge, *Dalton Trans.* **2007**, 4685–4692.
[29] H. Y. Chen, B. H. Huang, C. C. Lin, *Macromol.* **2005**, *38*, 5400–5405.
[30] G. R. Fulmer, A. J. M. Miller, N. H. Sherden, H. E. Gottlieb, A. Nudelman, B. M. Stoltz, J. E. Bercaw, K. I. Goldberg, M. Beckman, *Organometallics* **2010**, *29*, 2176–2179.
[31] E. Crosbie, A. R. Kennedy, R. E. Mulvey, S. D. Robertson, *Dalton Trans.* **2012**, *41*, 1832–1839.
[32] J. García-Álvarez, D. v. Graham, A. R. Kennedy, R. E. Mulvey, S. Weatherstone, *Chem. Commun.* **2006**, 3208–3210.
[33] S. Ghosh, D. Chakraborty, B. Varghese, *Eur. Polym. J.* **2015**, *62*, 51–65.
[34] N. T. Johnson, P. G. Waddell, W. Clegg, M. R. Probert, *Crystals* **2017**, *7*, 360.

Manuscript received: March 1, 2022
Revised manuscript received: March 29, 2022

# RESEARCH ARTICLE

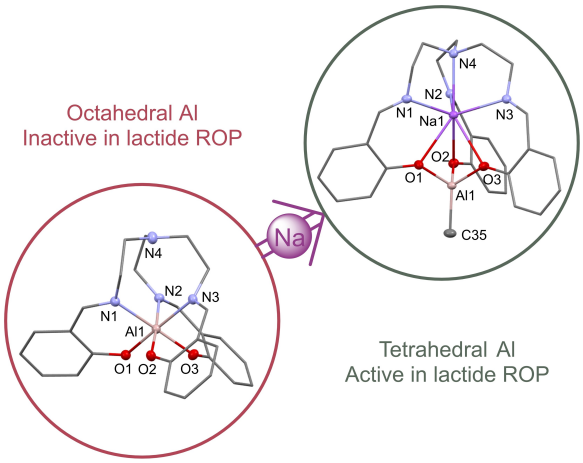


*Y. Zhou, Dr. G. S. Nichol, Dr. J. A. Garden**

1 – 9

**Incorporating Sodium to Boost the Activity of Aluminium TrenSal Complexes towards *rac*-Lactide Polymerisation**

Four novel homo- and heterometallic sodium and aluminium complexes based on the TrenSal ligand have been synthesised, characterised and tested in *rac*-lactide polymerisation. Reactivity studies indicated that the insertion of sodium to form heterometallic complexes alters the geometry of aluminium from octahedral to tetrahedral, switching from an inactive mono-Al complex to an active and controlled heterometallic catalyst for lactide polymerisation.